

The planar-to-tubular structural transition in boron clusters from optical absorption

Miguel A.L. Marques¹ and Silvana Botti²

¹*Institut de Minéralogie et de Physique des Milieux Condensés,*

Université Pierre et Marie Curie - Paris VI, 140 rue de Lourmel, 75015 Paris, France

²*Laboratoire des Solides Irradiés, CNRS-CEA-École Polytechnique, 91128 Palaiseau, France*

(Dated: November 11, 2018)

The optical response of the lowest energy isomers of the B_{20} family is calculated using time-dependent density functional theory within a real-space, real-time scheme. Significant differences are found among the absorption spectra of the clusters studied. We show that these differences can be easily related to changes in the overall geometry. Optical spectroscopy is thus an efficient tool to characterize the planar to tubular structural transition, known to be present in these boron based systems.

PACS numbers: 78.67.Bf, 64.70.Nd, 71.15.Mb

For the past years, boron nanostructures have attracted the attention of both theoretical and experimental physicists. This is due to the remarkable properties of boron, that make it an unique element in the periodic table, with important technological applications.^{1,2} Boron is characterized by a short covalent radius and has the tendency to form strong and directional chemical bonds.^{1,2} These characteristics lead to a large diversity of boron nanostructures – clusters,^{3,4,5,6,7} nanowires,⁸ and nanotubes^{9,10} – that have already been observed.

Many experimental studies of small boron-based clusters have been performed in the last decade, namely using mass and photo-electron spectroscopies.^{3,4,5,7} However, we still have very limited information regarding the geometries and electronic properties of these systems. From the theoretical point of view, there have been extensive *ab initio* quantum chemical and density functional calculations about the structural properties of neutral,^{3,5,7,11,12,13,14,15,16} cationic,^{15,17,18} and anionic clusters.^{5,7} The findings were fairly surprising. In fact, bulk boron appears in several crystalline and amorphous phases, the best know of which are the α - and β -rhombohedral, and the α -tetragonal, also known as low temperature or red boron. In these three phases, boron is arranged in B_{12} icosahedra^{1,19,20} (in the α -tetragonal phase these icosahedra are slightly distorted). However, the small clusters appear in four distinct shapes:¹⁶ convex, spherical, quasi-planar, and nanotubular – totally unrelated to the B_{12} icosahedra.

The most stable members of the B_n family with $n \lesssim 20$ are known to be planar.^{3,5,11,12,13,14,15} Recent calculations showed that B_n clusters with $n = 24$ and $n = 32$ prefer tubular structures.¹⁶ In a recent study⁷ Kiran *et al.* placed the transition between these two topologies at $n = 20$. However, their results were not totally conclusive: while the theoretical calculations (using density functional theory at the B3LYP/6-311+G* level) yielded a double ring arrangement as the lowest energy isomer of B_{20} and B_{20}^- , the experimental photo-electron spectra of anionic aggregates of the same size were only compatible with planar structures. Such a incongruity can be explained by the difficulties associated both to the

experimental and numerical techniques. Experimentally, the clusters were produced by laser evaporation of a disk target, with the formation of the fragments being mainly controlled by kinematics. The situation is similar, e.g., to the case of C_{20} : while the rings are easily produced by laser evaporation, the apparently more stable bowl and cage arrangements do not form spontaneously, but can only be obtained by fairly sophisticated chemical techniques.²¹ On the other hand, the theoretical determination of the lowest energy isomer is a very arduous task to current computational material science. The reason is twofold: i) with increasing number of atoms the number of metastable isomers increases exponentially; ii) and often the energy difference between competing structures becomes quite small. In the case of B_{20}^- , e.g., the four lowest lying isomers are separated by less than 0.3 eV (15 meV per atom).⁷ Clearly, this precision is beyond current density functional and quantum chemical methods for systems of this size. Once again, C_{20} is an illustrative example: to unveil its elusive ground state, scientists have tried density functional theory at various levels,^{22,23} quantum Monte Carlo,²² coupled cluster,²⁴ etc., without reaching any agreement regarding the energy ordering of the isomers.

In view of this situation, instead of relying on a single number, i.e., the total energy, in order to characterize a system, it is better to resort to the several spectroscopic tools available to both computational and experimental physics. It was, for example, the case of C_{20} , where the bowl and the cage isomers were identified by comparing the vibronic fine structures in photo-electron spectra with numerical calculations.²⁵ In this paper we propose the use of another spectroscopic tool, namely optical absorption, to provide clear signatures of the distinct B_{20} isomers. In fact, when the orbitals involved in the optical transitions are quite extended, as in the case of these boron clusters, optical spectroscopy in the visible and near-ultraviolet (near-UV) range turns out to be a rather sensitive probe of the overall shape of the system. In contrast to total energy differences, the absorption spectra are usually quite insensitive to small changes in the geometry, to the parametrization used for

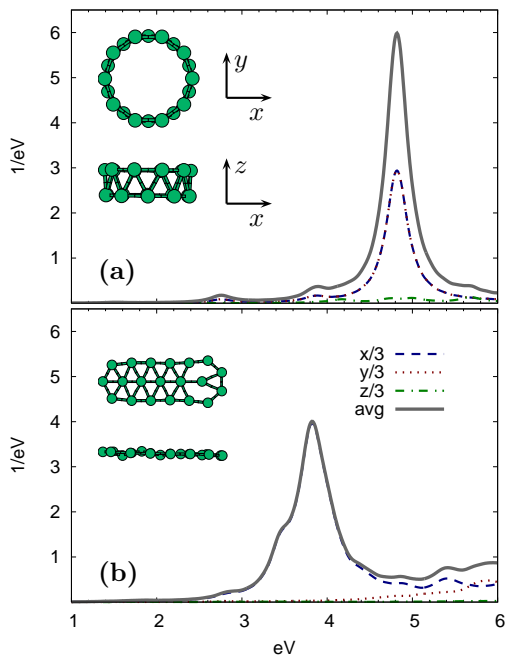


FIG. 1: (Color online) Dipole strength function for the different isomers of B_{20} . The corresponding geometries are shown in each panel. The gray (solid) line represents the absorption averaged over the three polarization directions; the blue (dashed), the red (dotted), and the green (dashed-dotted) lines indicate, respectively, the absorption in the x , y , and z directions. (These three last curves have been divided by 3.) The reference frame used is depicted in the top panel.

the exchange-correlation potential, and to changes in the pseudopotentials. This makes this tool valuable in studying structural transitions.

Our procedure relies on density functional theory and is briefly explained in the following. The geometries were optimized with the computer code *siesta*,³³ employing a double ζ with polarization basis set. From the optimized geometries, we then obtain the optical spectra within time-dependent density functional theory (TDDFT) in real time, as implemented in the computer code *octopus*,²⁷ using the PBE parametrization³⁴ in the adiabatic approximation for the exchange-correlation potential. For a technical description of this method we refer to Refs. 27 and 28. This approach has already been used for the study of metal and semi-conducting clusters,^{28,29} aromatic molecules,³⁰ protein chromophores,³¹ etc. Moreover, it proved quite successful in distinguishing the different isomers of C_{20} .³² When experimental spectra were available for a direct comparison, TDDFT within an adiabatic local density (LDA) or an adiabatic generalized gradient (GGA) approximation to the exchange-correlation functional reproduced the low energy peaks of the optical spectra with an accuracy of 0.1 eV.²⁸ This is in contrast with taking the differences of the eigenvalues of the HOMO and LUMO orbitals, which would give peaks at lower frequencies in

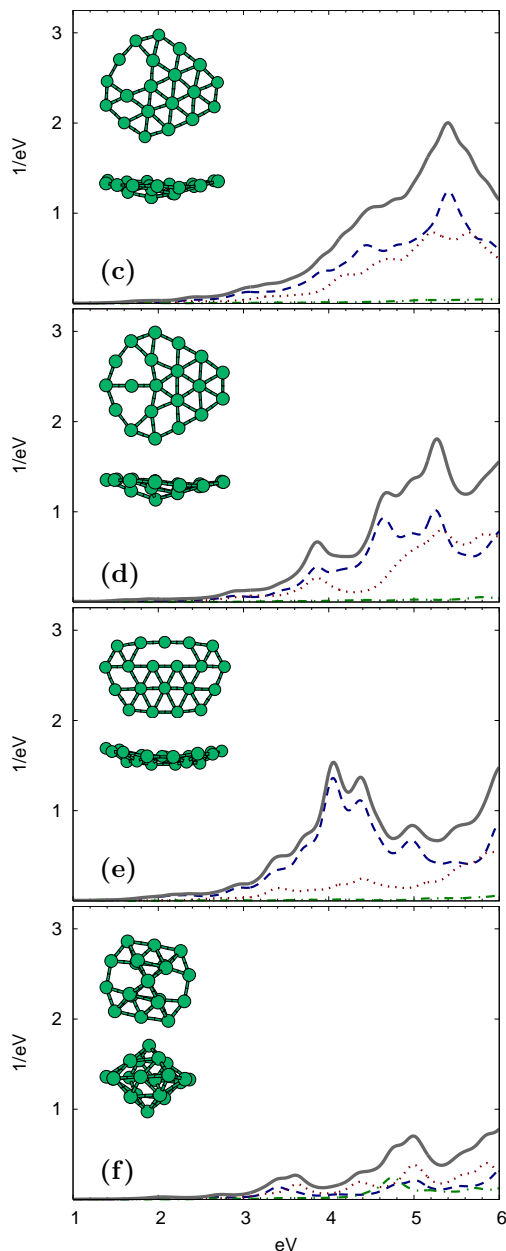


FIG. 2: (Color online) The same as Fig. 1 for the rest of the members of the B_{20} family studied in this work. Note the different vertical scale with respect to Fig. 1.

disagreement with the experimental spectra.³²

To represent the wave-functions in real space we used a uniform grid with a spacing of 0.23 Å, and a box extending 5 Å from the outer nuclear positions. A time step of 0.0013 fs assures the stability of the time propagation, and a total propagation time of 24.5 fs allows a resolution of about 0.1 eV in the resulting spectrum.

The isomers of B_{20} considered in this work can be divided in three broad categories (see Figs. 1 and 2): **a** – a nanotubular structure; **b** to **e** – quasi-two dimensional (2D) clusters; and **f** – a three dimensional (3D)

cage, that we obtained through a minimization procedure starting from a dodecahedron (a B_{20} fullerene-like structure). The geometries that we selected include the lowest energy isomers found in Ref. 7. Furthermore, we decided to add the cage isomer **f**, in order to reach more general conclusions on the effects of the 2D-to-3D transition on the optical response.

Total energies calculated at the relaxed geometries both with *siesta*³³ and *octopus*²⁷ confirm that the tubular structure **a** is the lowest lying isomer of the B_{20} . This is in agreement with the previous findings of Ref. 7, obtained using a B3LYP functional and a Gaussian basis set. In our calculation then follow isomers **c** ($\Delta E=0.43$ eV), **d** ($\Delta E=0.54$ eV), **f** ($\Delta E=0.62$ eV), **b** ($\Delta E=0.81$ eV), and **e** ($\Delta E=0.91$ eV). Note that the ordering is consistent with the one proposed in Ref. 7, except for cluster **f**, which was not considered in Ref. 7 as a low energy candidate for B_{20} . This discordance can be attributed to the basis set used in Ref. 7, or to the changes in the exchange-correlation functionals or pseudopotentials. Once again this reveals the danger of relying solely on the total energy to characterize such structural transitions.

The results of our calculations are summarized in Figs. 1 and 2, where we plot the computed dipole strength for six low-lying members of the B_{20} family. Besides the absorption spectra averaged over the three polarization directions (solid gray lines), we also depict the three components for light polarized along the Cartesian axis (see Fig. 1 **a** for the definition of the axis).

From the observation of Figs. 1 and 2, it is clear that the isomers of B_{20} have strikingly different absorption properties in the visible and near-UV, the range most easily accessible by experimental techniques. The tubular cluster **a** exhibits a large sharp peak at 4.8 eV, and two small peaks at around 2.7 and 3.9 eV. Also the quasi-planar isomer **b** absorbs light at well defined frequencies, with a main peak at 3.8 eV and a shoulder at 3.5 eV. The other quasi-2D structures **c**, **d**, and **e** no longer exhibit sharp peaks, but instead present broad features. This is easily explained by noting that these clusters have a larger distribution of bond lengths, due to the lack of symmetry around the boron centers. This is particularly evident in isomer **c**, resulting in an almost structureless spectrum that grows monotonically until around 5.4 eV. Nevertheless, the differences between these three spectra are still sufficient to distinguish among them: cluster **d** has a well defined peak at 3.9 eV, and the double peak at 4.0 and 4.4 eV is a clear signature of cluster **e**. Isomer **f** absorbs weakly visible and near-UV light. All quasi-2D isomers do not show any appreciable response for light polarization perpendicular to their plane; moreover, the response is stronger along the direction in which the cluster is more extended. Also in the case in which the plane is rolled up to form a tube, the contributions to the peaks come almost exclusively from absorption of light polarized perpendicularly to the axis of the tube.

In order to understand better the absorption in the

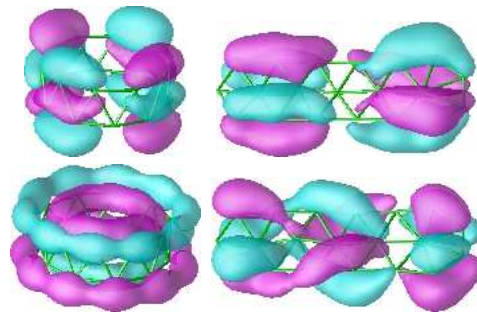


FIG. 3: (Color online) HOMO (top) and LUMO (bottom) states of the isomers **a** (left) and **b** (right). The magenta (cyan) isosurface corresponds to the positive (negative) part of the wave-functions.

planar and tubular isomers, we can learn from the shape of the Kohn-Sham orbitals (see Fig. 3). Both the HOMO and the LUMO, and several other states relevant to absorption, have predominantly π symmetry (with some σ admixture due to the breaking of planarity, which is particularly important in the case of the tubular shape). In this kind of compounds, the optical gap decreases with increasing length of the π system, and consequent increase of delocalization of the valence electrons. This is exactly what we observe in our spectra of planarlike isomers: isomer **b**, extending to almost 10 Å in the x direction absorbs at the lowest energy, followed by isomer **e**, and finally **c** and **d**. As already mentioned, these isomers are almost transparent for light polarized perpendicular to the plane (z direction in the figure). In fact, the light polarized in the z direction cannot excite the $\pi-\pi^*$ transitions and thus gives an almost negligible contribution to the spectra. In isomer **a**, there is a stronger contribution of the σ bonds to the relevant orbitals due to the curvature of the tube wall (see Fig. 3), which induces a considerable blue-shift of the main peak. Finally, we discuss the 3D cage **f** (see Fig. 2). As its bonds have a predominantly σ character, it does not exhibit strong absorption below 6 eV. As in the case of the irregular quasi-2D clusters, the large number of inequivalent boron atoms is responsible for the absence of well defined peaks.

The present results for B_{20} , together with the analogous results for C_{20} isomers,³² lead to some conclusions of wider validity. Two factors contribute to the position of the peaks and the overall shape of the spectra: i) the extension of the π system, which is directly related to the dimensionality and basic geometry of the cluster, determines the frequencies of strong absorption; and ii) the distribution of bond-lengths, related to the number of inequivalent boron atoms, determines if the spectrum is composed of sharp peaks or broad features. These factors are quite general, and are thus expected to apply to boron clusters of different sizes and any other class of clusters with similar chemical bonds.

In conclusion, we have shown how optical spectroscopy can be used to distinguish without ambiguity between the

different low-energy members of B_{20} family. The spectra in the visible and near-UV are very sensitive to the overall shape of the isomers. This is a general property that can be easily explained by simple geometrical arguments. In particular, the most stable neutral B_{20} isomer, i.e. the tubular cluster, can be unequivocally identified due to the presence of a very sharp resonance at about 4.8 eV. For this reason, we believe that optical spectroscopy can be an extremely efficient tool to study structural transitions in clusters. In the case of B_n aggregates, the comparison between experimental and computed absorption spectra, could bring a definitive answer to the unsolved question

of the critical size at which the transition between the planar and tubular structure occurs.

The authors would like to thank A. Castro, X. López, L. Reining, A. Rubio, and A. Seitsonen for useful suggestions and comments. MALM was supported by the Marie Curie Actions of the European Commission, Contract No. MEIF-CT-2004-010384. The authors also acknowledge partial support by the EC Network of Excellence NANOQUANTA (NMP4-CT-2004-500198). All computations were performed in the Laboratório de Computação Avançada of the University of Coimbra (Portugal).

-
- ¹ F. A. Cotton, G. Wilkinson, C. A. Murillo, and M. Bochmann, *Advanced Inorganic Chemistry*, 6th ed. Wiley, New York (1999).
- ² N. N. Greenwood and A. Earnshaw, *Chemistry of Elements*, 2nd ed. Butterworth-Heinemann, Oxford (1997).
- ³ L. Hanley, J. Witten, and S. L. Anderson, *J. Phys. Chem.* **92**, 5803 (1988).
- ⁴ S. J. La Placa, P. A. Roland, and J. J. Wynne, *Chem. Phys. Lett.* **190**, 163 (1992).
- ⁵ H.-J. Zhai, L.-S. Wang, A. N. Alexandrova and A. I. Boldyrev, *J. Chem. Phys.* **208**, 233 (2002).
- ⁶ H.-J. Zhai, A. N. Alexandrova, K. A. Birch, A. I. Boldyrev, and L.-S. Wang, *Angew. Chem. Int. Ed.* **42**, 6004 (2003); H.-J. Zhai, B. Kiran, J. Li and L.-S. Wang, *Nat. Mater.* **2**, 827 (2003).
- ⁷ B. Kiran, S. Bulusu, H.-J. Zhai, S. Yoo, X. C. Zeng, and L.-S. Wang, *Proc. Nat. Acad. Sci. USA* **102**, 961 (2005).
- ⁸ X. M. Meng, J. Q. Hu, Y. Jiang, C. S. Lee, and S. T. Lee *Chem. Phys. Lett.* **370**, 825 (2003).
- ⁹ I. Boustani, A. Quandt, E. Hernández, and A. Rubio *J. Chem. Phys.* **110**, 3176 (1999).
- ¹⁰ D. Ciuparu, R. F. Klie, Y. Zhu, and L. Pfefferle, *J. Phys. Chem. B* **108**, 3967 (2004).
- ¹¹ H. Kato and E. Tanaka, *J. Comput. Chem.* **12**, 1097 (1991); H. Kato and K. Yamashita, *Chem. Phys. Lett.* **190**, 361 (1992); H. Kato, K. Yamashita, and K. Morokuma, *Bull. Chem. Soc. Jpn.* **66**, 3358 (1993).
- ¹² A. K. Ray, I. A. Howard, and K. M. Kanal, *Phys. Rev. B* **45**, 14247 (1992).
- ¹³ A. C. Tang, Q. S. Li, C. W. Liu, and J. Li, *Chem. Phys. Lett.* **201**, 465 (1993).
- ¹⁴ I. Boustani, *Phys. Rev. B* **55**, 16426 (1997).
- ¹⁵ J. Niu, K. Rao, and P. Jena, *J. Chem. Phys.* **107**, 132 (1997).
- ¹⁶ I. Boustani, A. Rubio, and J. A. Alonso, *Chem. Phys. Lett.* **311**, 21 (1999); S. Chacko, D. G. Kanhere, and I. Boustani, *Phys. Rev. B* **68**, 035414-1 (2003).
- ¹⁷ I. Boustani, *Int. J. Quantum Chem.* **52**, 1081 (1994).
- ¹⁸ A. Ricca, C. W. Bauschlicher, *Chem. Phys.* **208**, 233 (1996).
- ¹⁹ C. L. Perkins, M. Trenary, and T. Tanaka, *Phys. Rev. Lett.* **77**, 4772 (1996).
- ²⁰ H. Hubert, B. Devouard, L. A. J. Garvie, M. O’Keeffe, P. R. Buseck, W. T. Petuskey, and P. F. McMillan, *Nature* **391**, 376 (1998).
- ²¹ H. Prinzbach, A. Weiler, P. Landenberger, F. Wahl, J. Wörth, L. T. Scott, M. Gelmont, D. Olevano and B. v. Issendorff, *Nature* **407**, 60 (2000).
- ²² J. C. Grossmann, L. Mitas and K. Raghavachari, *Phys. Rev. Lett.* **75**, 3870 (1995).
- ²³ R. O. Jones and G. Seifert, *Phys. Rev. Lett.* **79**, 443 (1997); K. Raghavachari, D. L. Strout, G. K. Odom, G. E. Scuseria, J. A. Pople, B. G. Johnson and P. M. W. Gill, *Chem. Phys. Lett.* **214**, 357 (1993).
- ²⁴ E. J. Bylaska, P. R. Taylor, R. Kawai and J. H. Weare, *J. Phys. Chem.* **100**, 6966 (1996).
- ²⁵ M. Saito and Y. Miyamoto, *Phys. Rev. Lett.* **87**, 035503 (2001).
- ²⁶ M. A. L. Marques and E. K. U. Gross, *Annu. Rev. Phys. Chem.* **55**, 427 (2004).
- ²⁷ M. A. L. Marques, A. Castro, G. F. Bertsch and A. Rubio, *Computer Phys. Commun.* **151**, 60 (2003). The code `octopus` is available at <http://www.tddft.org/programs/octopus/>.
- ²⁸ A. Castro, M. A. L. Marques, J. A. Alonso, and A. Rubio, *J. Comp. Theoret. Nanoscience* **1**, 231 (2004).
- ²⁹ M. A. L. Marques, A. Castro, and A. Rubio, *J. Chem. Phys.* **115**, 3006 (2001).
- ³⁰ K. Yabana and G. F. Bertsch, *Int. J. Quant. Chem.* **75**, 55 (1999); G. Mallocci, G. Mulas, and C. Joblan, *Astronomy & Astrophysics* **426**, 105 (2004); G. Mallocci, G. Mulas, G. Cappellini, V. Fiorentini, and I. Porceddu, *Astronomy & Astrophysics* **443**, 585 (2005).
- ³¹ M. A. L. Marques, X. López, D. Varsano, A. Castro, and A. Rubio, *Phys. Rev. Lett.* **90**, 258101 (2003); X. López, M. A. L. Marques, A. Castro, and A. Rubio, submitted (2005).
- ³² A. Castro, M. A. L. Marques, J. A. Alonso, G. F. Bertsch, K. Yabana, and A. Rubio, *J. Chem. Phys.* **116**, 1930 (2002).
- ³³ J. M. Soler, E. Artacho, J. D. Gale, A. García, J. Junquera, P. Ordejón, and D. Sánchez-Portal, *J. Phys.: Condens. Matter* **14**, 2745 (2002).
- ³⁴ J. P. Perdew, K. Burke, and M. Ernzerhof, *Phys. Rev. Lett.* **77**, 3865 (1996).